PHYSICAL REVIEW B VOLUME 49, NUMBER 8 15 FEBRUARY 1994-II

Second-order Raman spectroscopy of AlAs: A test of lattice-dynamical models

G. S. Spencer, J. Grant, R. Gray,* J. Zolman,† and J. Menéndez
Department of Physics, Arizona State University, Tempe, Arizona 85287-1504

R. Droopad and G. N. Maracas
Department of Electrical Engineering, Arizona State University, Tempe, Arizona 85287-5706
(Received 25 October 1993)

The second-order Raman spectrum of AlAs has been measured on samples grown by molecular-beam epitaxy (MBE). The results show significant discrepancies with model calculations of the phonon density of states, but are consistent with recent first-principles calculations. This first-principles approach has been used to compute the phonon energies in GaAs-AlAs superlattices, with controversial implications regarding the sharpness of MBE-grown interfaces. The Raman results presented here support the conclusions of the first-principles analysis.

GaAs, AlAs, and their alloys share a common anion, have nearly identical lattice constants, and possess very different band gaps. These attributes make them an ideal system for heteroepitaxy. Not surprisingly, great advances have been made in the fabrication of artificial structures such as GaAs-$Al_xGa_{1-x}As$ superlattices.[1] Some possible uses for these structures are devices such as tunable semiconductor lasers, solid-state photomultipliers, and graded gap transistors.[2] More recently, ultrathin GaAs-AlAs superlattices have attracted great interest.[3] In these superlattices layers of GaAs and AlAs as thin as a few atomic constants are alternated. This structure leads to a "folding" of the bulk phonon energy band and raises the possibility of band-gap engineering beyond the simple shift in band-gap energies obtained in thicker structures. The quality of ultrathin superlattices depends critically upon the flatness of the GaAs-AlAs interfaces present in the crystal. The possibility of fabricating such flat interfaces remains a controversial issue.[4–9] While some optical experiments have been traditionally interpreted in terms of atomically flat interfaces, more recent microscopy results suggest that roughness is present in superlattice samples.

Raman spectroscopy has been shown to be a sensitive tool for the characterization of the superlattice interface structure.[10–17] Due to the elastic mismatch between GaAs and AlAs, optical phonons in superlattices grown from these materials become confined. For a $(GaAs)_{n_1}(AlAs)_{n_2}$ superlattice there are $3n_1$ [n_1 longitudinal-optic (LO) and $2n_1$ transverse-optic (TO)] GaAs-like modes and $3n_2$ AlAs-like optic modes. The frequencies of these modes can be accurately predicted from the associated bulk dispersion relation $\omega(\mathbf{k})$ using an effective wave vector along the growth direction given by

$$k=\frac{m\pi}{(n_i+1)a}\ , \tag{1}$$

where m is the index of the mode (e.g., LO_m), and a is the layer spacing in the superlattice.[18] Due to the parabolically decreasing nature of the optical branches, superlattice mode energies are shifted downward with respect to the bulk LO-phonon energy. Deviations of the phonon frequency from those predicted by the bulk dispersion relation can be traced back to changes in the effective thickness of the layer n_i, or to changes in the bulk $\omega(\mathbf{k})$ due to alloying. The difficulty in separating the two effects and the lack of experimental values for $\omega(\mathbf{k})$ in AlAs have been a limiting factor for the use of Raman spectroscopy as a characterization tool of ultrathin superlattices.

Recently, Giannozzi *et al.* presented first-principles calculations of the phonon dispersion curves for tetrahedral semiconductors in remarkable agreement with existing experimental data.[19] While little experimental data exist for AlAs, the dispersion curves calculated by Giannozzi *et al.* for AlAs show noticeable differences from previous AlAs calculations. The most striking is the near flat nature of the LO branch along the (001) direction. When the bulk dispersion relation is not flat, as in the case of GaAs, the superlattice modes for $m=1,2,3$, etc. are well separated due to the downward nature of $\omega(\mathbf{k})$. Hence the Raman spectra of these GaAs-like optic modes in a superlattice is a series of distinct, well-separated peaks. If, however, the bulk dispersion relation is nearly flat, then there is little separation between modes. This is the case for AlAs according to Giannozzi *et al.* Therefore, the AlAs-like Raman peaks from a perfect GaAs-AlAs superlattice should be almost unshifted with respect to bulk AlAs.

While theory predicts no significant downward shift of the AlAs-like phonons in ultrathin superlattices, experiment has shown a substantial downward shift to exist in nearly all samples grown to date. Molinari *et al.* have used the first-principles results of Giannozzi *et al.* to explain these results.[20] The calculations of Molinari *et al.* show that the experimental Raman results for ultrathin superlattices cannot be explained without the inclusion of alloying at the interfaces. Due to the flatness of the cal-

culated AlAs dispersion relation, shifts in the AlAs-like optic mode frequencies with respect to bulk frequencies cannot be accounted for by a change in the effective thickness n_i in Eq. (1). However, as described in Ref. 20, the presence of Ga atoms in nominally pure Al planes reduces the effective charge of the mode, thereby lowering the mode frequency due to the reduced LO-TO splitting. Thus, the only possible explanation for the experimental downshifts is that in *virtually all structures fabricated to date, there is a considerable amount of cation interdiffusion.*

Since the conclusion from the work of Molinari *et al.* depends so critically on the flatness of the AlAs dispersion relation, the accuracy of the first-principles calculation is of extreme importance. Therefore, if the results of Giannozzi *et al.* are to be used in the characterization of superlattice interface structure, as in Ref. 20, further experimental verification is desirable. In order to confirm the calculated dispersion curves, it is necessary to measure phonon frequencies for different values of wave vector $\mathbf{k}$. So far, the only spectroscopic information on AlAs comes from first-order Raman scattering (limited to $\mathbf{k}=\mathbf{0}$) and phonon-assisted optical emission. From first-order Raman spectroscopy we obtain $\omega_{LO}(\Gamma)=404\pm1$ cm^{-1} and $\omega_{TO}(\Gamma)=361\pm1$ cm^{-1}. The optical emission experiments yield $\omega_{LO}(X)=403\pm8$ cm^{-1}, $\omega_{TO}(X)=335\pm8$ cm^{-1}, $\omega_{LA}(X)=222\pm12$ cm^{-1}, and $\omega_{TA}(X)=109\pm8$ cm^{-1}.[21] Here Γ represents $\mathbf{k}=\mathbf{0}$, and X represents $\mathbf{k}=2\pi/a(100)$. The calculated first-principles values for the above phonons [shown in Table I with the exception of LA(X)=215 cm^{-1}] are in excellent agreement with experiment, but more data are needed to confirm the calculated dispersion *curves* $\omega(\mathbf{k})$. The traditional source for these data is neutron scattering. However, due to current limitations in crystal size, neutron scattering results are not available. A less direct, but potentially very accurate method for verifying the calculated dispersion relation is to look at the associated density of states. In Fig. 1 three densities of states calculated by different means are plotted. Two are calculated using the rigid-ion model[22] and utilizing parameters fit by Ren, Chu, and Chang.[23] The first (bottom) uses parameters fit to theoretical calculations of Yip and Chang[24] and the second (middle) uses parameters fit to available AlAs experimental data.[25–27] The third (top) curve is the first-principle calculations performed by Giannozzi *et al.* Note the dissimilarity between the shapes of the calculated density of states (even though the models fit the available data very well), thus confirming the sensitivity of the density of states to the phonon dispersion relations.

The experimental tool to investigate the phonon density of states is second-order Raman scattering. This is a higher-order scattering process in which two phonons are generated whose combined wave vector adds up to zero. Thus, the individual phonon wave vector is no longer restricted, and phonons all the way through the Brillouin zone become Raman active. However, since second-order Raman scattering allows in principle the combination of any two phonons, provided they have opposite wave vectors, the resulting spectrum will not resemble the phonon density of states unless the two-phonon combination is restricted to phonons belonging to the same branch. To an excellent approximation, this can be achieved experimentally by performing the experiment in the *polarized* configuration (parallel incident and scattered polarizations).[28] Under these conditions, the second-order Raman spectrum is approximately proportional to the phonon density of states (except for an obvious scaling by a factor of 2 in the frequency axis) times a function of the frequency that takes into account matrix elements and phonon occupation. By making simple assumptions concerning matrix elements, the multiplicative function can be written as $\{[n(\omega)+1]/\omega\}^2$,[28] where $n(\omega)$ is the phonon occupation number. Due to these approximations, the polarized second-order Raman spectrum will be similar but not identical to the phonon density of states. However, the difference between the densi-

TABLE I. Positions of AlAs peaks indicated by dashed lines in Figs. 2 and 3 are tabulated. Density-of-states peak positions are from first-principles calculations of Giannozzi *et al.* The experimental second-order Raman peak positions have been divided by 2 for direct comparison with the density-of-states calculation. Note excellent agreement, especially for higher-energy modes. Peak positions in parentheses are from first-order Raman scattering.

Peak	Density of states position (cm^{-1})	Experimental position/2 (cm^{-1})	Absolute difference (cm^{-1})	Percent difference (%)
TA(L)?[a]	71?	82	11?	13.4?
TA(X)	95	103	8	7.7
TO(X)	337	340	3	0.9
TO(L)	352	350	2	0.6
TO(Γ)	363	366(361)	3(2)	0.8(0.5)
LO(X)	393	400	7	1.8
LO(Γ)	400	409(404)	9(4)	2.2(1.0)

[a]Mode attributed to the AlAs TA(L) might be the GaAs TA(X) mode from the substrate and cap which is found at 79 cm^{-1}. It is included here for completeness.

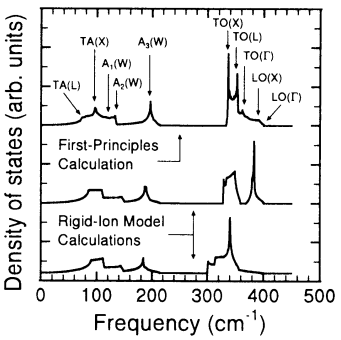

FIG. 1. Three calculated density-of-states curves for AlAs. The bottom two are calculated using the rigid-ion model. Parameters for the bottom curve are fit to theoretical calculations of Yip and Chang while those for the middle curve are fit to available AlAs experimental results. Both sets of parameters were fit by Ren, Chu, and Chang. The top curve is the first-principles calculation for the density of states by Giannozi *et al.* with phonon type and positions indicated.

ties of states in Fig. 1 is so pronounced, particularly in the optic range, that we expect the second-order Raman spectrum to help us decide which theoretical approach best represents the phonon dispersion curves. In addition, the position of critical points, which lead to very sharp structures in the density of states, will not be affected by the matrix-element effects. The study of these critical points allows the determination of single-phonon frequencies and provides an invaluable tool for the assessment of the theoretical calculations.

A complication of experimental nature arises when one attempts to measure a second-order Raman spectrum. Since it is a second-order process, its intensity is much weaker (~ 50 times for AlAs) than the intensity of first-order scattering. To lessen the first-order dominance, we used the scattering configuration $z(x,x)\bar{z}$ [incident wave vector along z, scattered wave vector along $\bar{z}$, incident and scattered light polarized along x, with $x=(100)$, and $z=(001)$] in which the first-order mode is forbidden.

The investigated sample was grown by molecular-beam epitaxy in a Varian Gen II system. A 0.5-μm layer of AlAs was deposited on a GaAs substrate and capped with a 40-Å layer of GaAs to prevent oxidation. Raman experiments were performed at low temperature ($T=36$ K) for comparison with the low-temperature density-of-states calculations. The scattering configuration employed was $z(x,x)\bar{z}$, using discrete Ar^+ and Kr^+ laser lines. The scattered light was dispersed by a SPEX 1877 triple spectrometer and detected using a SPEX CCD optical multichannel analyzer.

In Figs. 2 and 3 our experimental second-order Raman spectra are plotted with the first-principles calculated density of states (the intensity has been multiplied by $\{[n(\omega)+1]/\omega\}^2$ and the Raman shift scaled by 2) in the ranges of 100–300 and 650–850 cm^{-1}, respectively. The second-order Raman spectrum in the range 300–650 cm^{-1} is not displayed due to the dominant GaAs modes from the cap and substrate layers. Although one cannot expect the second-order Raman spectrum to look exactly

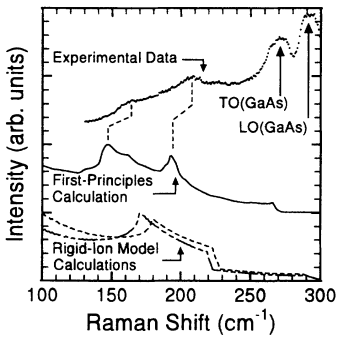

FIG. 2. Polarized, second-order Raman (low-temperature) results are compared with density-of-states calculations for AlAs low-energy modes. The density-of-states intensities have been multiplied by $\{[n(\omega)+1]/\omega\}^2$ and Raman shifts have been scaled by 2 for direct comparison with experimental results. Peak positions indicated by dashed lines are tabulated in Table I. The middle (solid) curve is the first-principles density of states calculated by Giannozzi *et al.* The two dashed (bottom) curves are the rigid-ion model calculated density of states plotted for reference.

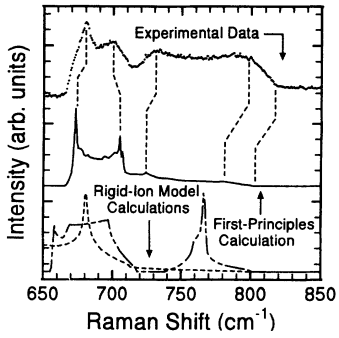

FIG. 3. Polarized, second-order Raman (low-temperature) results are compared with density-of-states calculations for AlAs high-energy modes. The density-of-states intensities have been multipled by $\{[n(\omega)+1]/\omega\}^2$ and Raman shifts have been scaled by 2 for direct comparison with experimental results. Peak positions indicated by dashed lines are tabulated in Table I. The middle (solid) curve is the first-principles density of states calculated by Giannozzi *et al.* The two dashed (bottom) curves are the rigid-ion model calculated density of states plotted for reference.

like the density of states for the previously mentioned reasons, examination of Figs. 2 and 3 shows the overall shape of the first-principles density of states and the second-order data to be consistent. Neither of the rigid-ion model calculations using the parameters of Ren, Chu, and Chang are found to be in good agreement with experiment. (Also plotted in Figs. 2 and 3 for reference.) Table I contains the second-order Raman peak positions and the corresponding first-principles critical point energies and assignments.[29] The second-order Raman peak positions have been divided by a factor of 2. Also given in Table I are the first-order Raman results for the Γ-point phonons. The difference between the first- and second-order frequencies are due to instrumental error and the difficulty in assigning positions in the second-order spectrum. The agreement of the first-principles calculation with both first- and second-order Raman experiments is excellent, particularly for the optical branches, where often the measured and calculated critical points differ by less than 1%; a remarkable result for a first-principles calculation. For the acoustic branches, the discrepancies are somewhat larger, but in the case of the largest disagreement [the TA(L) mode at 82 cm^{-1}] we suspect that we might actually be measuring the TA(X) phonon of the GaAs cap and substrate layers, which has been calculated by Giannozzi *et al.* to be at precisely 82 cm^{-1} and previously found experimentally at 79 cm^{-1}.[30] Even if we admit that the acoustic branches are somewhat less accurate, however, it is apparent that the use of the first-principles approach to model *optical* branches in GaAs-Alas superlattices is fully justified.

Another test of the calculated density of states is the separation between the energies of the LO phonon at the Γ and the X points. This is, after all, a measure of the "flatness" of the LO branch of the dispersion curve. The results of Giannozzi *et al.* show this separation to be 7 cm^{-1}. We found the separation between the experimental LO (Γ) and LO(X) (from second-order data in Table

I) modes to be 9 cm^{-1}. However, when we convolute the theoretical density of states with the experimental resolution function, we obtain a predicted separation of 10 cm^{-1}. Hence the agreement is excellent within experimental error.

In conclusion, we find the second-order Raman spectra to be in close agreement with the first-principles density of states calculated by Giannozzi *et al.* Since the density of states is so intimately related to the dispersion curves, this confirms that the phonon dispersion curves obtained from first-principles calculations are extremely accurate. Using the dispersion relation of Giannozzi *et al.*, superlattice samples grown at traditional fabrication temperatures of 500 °C or more can be shown to have significant alloying. However, recent results indicate that low growth temperature samples ($T_g = 350$ °C) have much better agreement with theoretical calculations for a perfect superlattice.[31]

We wish to thank Paolo Giannozzi and Stefano Baroni for many helpful discussions, and for making their numerical results and figures available to us. The critical point analysis shown in the top graphic of Fig. 1 is due to Pasquale Pavone, Wolfgang Windl, and Stefano Baroni. Some of this work was performed under the auspices of the Arizona State University Physics Research Experience for Undergraduates Program; sponsored by the National Science Foundation under Grant No. DMR 92-00055, and Arizona State University. This work has also been supported by the National Science Foundation under Grants Nos. DMR-88-14918 and DMR 91-21567.

---

*Present address: Physics Department, Alma College, Alma, MI 48801.

†Present address: Physics Department, Kenyon College, Gambier, OH 43022.

[1]For a review, see E. O. Göbel and K. Ploog, Prog. Quantum Electron. **14**, 289 (1990).

[2]For a review, see F. Capasso, Science **235**, 172 (1987); F. Capasso, K. Mohammed, and A. Y. Cho, IEEE J. Quantum Electron. **QE-22**, 1853 (1986).

[3]L. J. Sham and Y.-T. Lu, J. Lumin. **44**, 207 (1989), and references therein.

[4]A. Ourmazd, D. W. Taylor, J. Cunningham, and C. W. Tu, Phys. Rev. Lett. **62**, 933 (1989).

[5]B. Deveaud, B. Guenais, A. Pouloulec, A. Regreny, and C. d'Anterroches, Phys. Rev. Lett. **65**, 2317 (1990).

[6]A. Ourmazd and J. Cunningham, Phys. Rev. Lett. **65**, 2318 (1990).

[7]L. Pfeiffer, E. F. Schubert, K. W. West, and C. W. Magee, Appl. Phys. Lett. **58**, 2258 (1991).

[8]R. Köhrbrück, S. Munnix, D. Bimberg, D. E. Mars, and J. N. Miller, J. Vac. Sci. Technol. B **8**, 798 (1990).

[9]U. Meirav, M. Heiblum, and F. Stern, Appl. Phys. Lett. **52**, 1268 (1988).

[10]J. Sapriel, J. C. Michel, J. C. Tolédano, R. Vacher, J. Kervarec, and A. Regreny, Phys. Rev. B **28**, 2007 (1983).

[11]K. Kubota, N. Nakayama, H. Katoh, and N. Sano, Solid State Commun. **49**, 157 (1984).

[12]M. V. Klein, C. Colvard, R. Fischer, and H. Morkoç, J. Phys. C **5**, 131 (1984).

[13]B. Jusserand, F. Alexandre, D. Paquet, and G. Le Roux, Appl. Phys. Lett. **47**, 301 (1985).

[14]D. Levi, Shu-Lin Zhang, M. V. Klein, J. Klem, and H. Morkoç, Phys. Rev. B **36**, 8032 (1987).

[15]G. Fasol, M. Tanaka, H. Sakaki, and Y. Horikoshi, Phys. Rev. B **38**, 6056 (1988).

[16]B. Jusserand, F. Mollot, J.-M. Moisson, and G. Le Roux, Appl. Phys. Lett. **57**, 560 (1990).

[17]N. Hara and T. Katoda, J. Appl. Phys. **69**, 2112 (1991).

[18]For reviews, see M. V. Klein, IEEE J. Quantum Electron. **QE-22**, 1760 (1986); B. Jusserand and M. Cardona, in *Light Scattering in Solids V,* edited by M. Cardona and G. Güntherodt (Springer, Berlin, 1989); J. Menéndez, J. Lumin. **44**, 285 (1989).

[19]P. Giannozzi, S. de Gironcoli, P. Pavone, and S. Baroni, Phys. Rev. B **43**, 7238 (1991).

[20]E. Molinari, S. Baroni, P. Giannozzi, and S. de Gironcoli, Phys. Rev. B **45**, 4280 (1992).

[21]B. Monemar, Phys. Rev. B **8**, 5711 (1973).

[22]K. Kunc, M. Balkanski, and M. A. Nusimovici, Phys. Rev. B **12**, 4346 (1975).

[23]S. F. Ren, H. Chu, and Y. C. Chang, Phys. Rev. B **37**, 8899 (1988).

[24]S. K. Yip and Y. C. Chang, Phys. Rev. B **30**, 7037 (1984).

[25]C. Colvard, R. Merlin, M. V. Klein, and A. C. Gossard, Phys. Rev. Lett. **45**, 298 (1980).

[26]A. S. Barker, Jr., J. L. Merz, and A. C. Gossard, Phys. Rev. B **17**, 3181 (1978).

[27]M. Ilegems and G. L. Pearson, Phys. Rev. B **1**, 1576 (1970).

[28]*Light Scattering in Solids II,* edited by M. Cardona and G. Güntherodt, Topics in Applied Physics Vol. 50 (Springer, Berlin, 1983), p. 39.

[29]P. Pavone, W. Windl, and S. Baroni (private communication).

[30]R. Trommer and M. Cardona, Phys. Rev. B **17**, 1865 (1978).

[31]G. S. Spencer, J. Menéndez, J. Grant, L. N. Pfeiffer, and K. W. West (unpublished).